Experiments in Fluids 21 (1996) 218–226 © Springer-Verlag 1996

Reynolds-number-dependence of the maximum in the streamwise velocity fluctuations in wall turbulence

S. Mochizuki, F. T. M. Nieuwstadt

Abstract A survey is made of the standard deviation of the streamwise velocity fluctuations in near-wall turbulence and in particular of the Reynolds-number-dependency of its peak value. The following canonical flow geometries are considered: an incompressible turbulent boundary layer under zero pressure gradient, a fully developed two-dimensional channel and a cylindrical pipe flow. Data were collected from 47 independent experimental and numerical studies, which cover a Reynolds number range of $R_\theta = U_\infty \theta/\nu = 300$–$20{,}920$ for the boundary layer with θ the momentum thickness and $R^+ = u_* R/\nu = 100$–$4{,}300$ for the internal flows with R the pipe radius or the channel half-width. It is found that the peak value of the rms-value normalised by the friction velocity, u_*, is within statistical errors independent of the Reynolds number. The most probable value for this parameter was found to be 2.71 ± 0.14 and 2.70 ± 0.09 for the case of a boundary layer and an internal flow, respectively. The present survey also includes some data of the streamwise velocity fluctuations measured over a riblet surface. We find no significant difference in magnitude of the normalised peak value between the riblet and smooth surfaces and this property of the normalised peak value may for instance be exploited to estimate the wall shear stress from the streamwise velocity fluctuations. We also consider the skewness of the streamwise velocity fluctuations and find its value to be close to zero at the position where the variance has its peak value. This is explained with help of the equations of the third-order moment of velocity fluctuations. These results for the peak value of the rms of the streamwise velocity fluctuations and also the coincidence of this peak with the zero value of the third moment can be interpreted as confirmation of local equilibrium in the near-wall layer, which is the basis of inner-layer scaling. Furthermore, these results can be also used as a requirement which turbulence models for the second and triple velocity correlations should satisfy.

Received: 20 December 1995/Accepted: 13 March 1996

S. Mochizuki[1], F. T. M. Nieuwstadt
Laboratory for Aero and Hydrodynamics
Delft University of Technology
NL-2628 AL Delft, The Netherlands

Correspondence to: F. T. M. Nieuwstadt

[1]*Present address*: Yamaguchi University, Tokiwadai Ube 755, Japan

The authors are indebted to Prof. P. Bradshaw for making available his list of references on this topic and for his remarks on "active" and "inactive" motions. We also gratefully acknowledge discussions with Prof. I. Castro regarding the value of σ_u^+ above rough walls.

1 Introduction

The Reynolds number is a fundamental parameter in fluid mechanics which describes the ratio of inertial to viscous effects in a flow. When the Reynolds number is low, viscous forces dominate and the flow is so-called laminar. On the other hand, when the Reynolds number exceeds a certain threshold the laminar flow becomes unstable and a transition occurs to turbulent flow. When in the latter case the Reynolds number becomes sufficiently high, one speaks of fully-developed turbulence. The large-scale characteristics of the flow, such as the variances of the velocity fluctuations, become then independent of the Reynolds number. This condition is known as Reynolds-number similarity (Tennekes and Lumley 1972, p. 6).

However, between transition and fully developed turbulence there is a range, where the flow variables depend in general on the Reynolds number. This dependence on Reynolds number plays for instance a role when one tries to extrapolate small-scale experimental results to real-size applications. The experiments are usually carried out in the laboratory under low-Reynolds number conditions, whereas the practical applications of the same flow occur mostly at high Reynolds numbers. To make the step from experiments to real applications, information is required on the Reynolds dependency of turbulence variables in various flow geometries. Several studies have been already carried out on this subject and we may refer to Gad-el-Hak and Bandyopadhyay (1994) for a recent review. In this study we will concentrate on the Reynolds dependency of one particular turbulence variable, i.e. the streamwise velocity fluctuations in near-wall turbulence.

To obtain data for these near-wall streamwise velocity fluctuations, we turn to two sources. The first is Direct Numerical Simulation (DNS). DNS is nowadays a well-established tool to study turbulence and it provides detailed information on the turbulence flow field (Kim et al. 1987; Spalart 1988; Eggels et al. 1994). DNS has contributed considerably to our knowledge of turbulence in various flow geometries. Its disadvantage, however, is that it can be used only for rather small Reynolds numbers.

The second source of data is laboratory experiments. A large number of experiments are available in the literature on the canonical flow geometries that we will study here and for a review we may again refer to Gad-el-Hak and Bandyopadhyay

(1994). However, a few examples deserve to be mentioned here: for instance, the extensive survey of mean velocity data in a turbulent boundary layer that was made by Coles (1956) and based on which he proposed the law of the wake. Another experimental study of the turbulent boundary layer was performed by Murlis et al. (1981). Dean (1978) investigated experimental data obtained in two-dimensional channel flows. He determined the Reynolds-number-independent log-law constants and applied law of the wake to this internal flow. In the more recent experiments use was made of laser doppler anemometry (LDA) which can realize quite high spatial resolution and which is able to measure instantaneous velocity statistics in the viscous sublayer close to the wall (Karlsson and Johansson 1988; Fontaine and Deutsch 1995; Ching et al. 1995; Durst et al. 1995). For instance, Wei and Willmarth (1989) carried out LDA measurements in a two-dimensional channel flow over a wide range of Reynolds numbers, $R_D = 3{,}850$–$230{,}000$. They pointed out that the inner-layer scaling fails to show similarity in Reynolds-stress profiles in the inner layer. Antonia et al. (1992) studied low-Reynolds-number effects in fully developed turbulent channel flow with data obtained both from experiments and DNS. A similar study has been performed for the boundary layer by Ching et al. (1995) and for the cylindrical pipe flow by den Toonder and Nieuwstadt (1996). These studies show that only at high enough Reynolds number, turbulent statistics in terms of inner-layer scaling appear to obey Reynolds-number similarity in the upper part of the viscous sublayer and in the buffer layer (for further discussion see also Dussauge et al. 1995).

In the present study we focus on the peak value of streamwise velocity fluctuations in wall turbulence. We investigate the Reynolds-number-dependency of this parameter for a number of canonical flow geometries, i.e. a zero-pressure-gradient boundary layer, a two-dimensional channel and a cylindrical pipe. The data are obtained from laboratory experiments and DNS in a wide range of Reynolds numbers. In addition we consider the value of the third-order moment (skewness) at the position where the peak in the rms value occurs. The study was motivated by some recent results (Ching et al. 1995; Durst et al. 1995) in which only a weak Reynolds-number-dependency of this peak value was found. Here we aim to extend these findings to a larger range of Reynolds numbers in order to establish whether the maximum value of the streamwise velocity fluctuations can indeed be considered as Reynolds number independent. Moreover, we aim to investigate whether this peak value is independent of flow geometry by comparing data for various types of wall-bounded turbulent flows. In case the Reynolds independency is found to be true, this would have important implications, e.g. for near-wall scaling and for turbulence modelling. However, this result could also be used to estimate the wall shear stress from observations of the streamwise velocity fluctuations.

The organization of the paper is as follows. First we review shortly the data on which our study is based. Then we analyze the peak value of the root-mean-square (rms) of the streamwise velocity fluctuations as function of Reynolds number. The analysis is subdivided according to flow geometries, i.e. external versus internal flows. Next we consider the skewness of the streamwise velocity fluctuations at the position of the peak of the rms. The influence of measuring resolution is also considered and we finish our study with a summary and conclusions.

2
Data collection

The peak value of the rms of the streamwise velocity fluctuations and the third-order moment of these fluctuations at the position of the rms-peak were collected from 42 independent experimental and direct simulation data. A summary of all data sources together with some additional details is given in Tables 1 and 2. The flow geometries are an incompressible, two-dimensional turbulent boundary layer under zero pressure gradient, which is a streamwise developing flow and a fully developed two-dimensional channel and cylindrical pipe flow which are independent of the streamwise coordinate. For the flows given in Table 1, the wall can be considered as smooth. For the boundary-layer case no separate distinction is made according the free-stream turbulence level because no significant change in the peak value was found for a free-stream turbulence up to 1.8%. Moreover, a possible influence of the free-stream turbulence level is still unknown (Gad-el-Hak and Bandyopadhyay 1994).

Apart from data over smooth walls, we also consider in this study some experiments carried out over a riblet surface. These experiments are given in Table 2. Riblets are small longitudinal grooves in the wall parallel to the mean flow and they are known to cause skin-friction reduction (e.g. deBisschop and Nieuwstadt 1996).

3
Peak value of σ_u^+

Let us consider the streamwise velocity fluctuations in a near-wall turbulent flow. The σ_u^+ denotes the standard deviation or the rms-value of these fluctuations normalized with the friction velocity u_* where u_* is defined as $u_* \equiv \sqrt{\tau_w/\rho}$ with τ_w the wall shear stress and ρ the fluid density. It should be stressed here that an accurate estimate of the u_* is very important for our analysis. Therefore, we have entered in the Tables 1 and 2 the method by which u_* was obtained in the various experiments. We can distinguish so-called direct and indirect methods.

As direct methods to determine the wall shear stress, we can classify the pressure-drop measurement (only applicable in pipe flow) and the measurement with a drag balance. These methods, especially in the case of a drag balance, are rather difficult from an experimental point of view.

As indirect methods we classify all procedures based on the use of the linear or logarithmic velocity profile and also the Preston-tube observations. Durst et al. (1996) show that the procedure based on adoption of a linear velocity profile can lead to substantial errors unless measurements very close to the wall are taken. In case of the procedure using the logarithmic profile, a choice has to be made for the log-law constants. Various values for these constants have been proposed (Hinze 1975, p. 626). Blackwelder and Haritonidis (1983) noted that the friction velocity obtained using a universal log-law is typically 15% greater than the value obtained by using the linear profile in the viscous sublayer.

Table 1. References of data over a smooth wall. Apart from the source, we also indicate in the vertical columns the following variables: The experimental method (HWA: hot-wire anemometry; LDA: Laser-Doppler anemometry; DNS: direct numerical simulation); The measuring method for the wall shear stress: ($U^+ = y^+$: use the linear velocity law near the wall); Log-law (A, B) (the use of the logarithmic velocity profile with the constants $U^+ = A \log y^+ + B$); Preston tube, Pressure-drop measurement; Drag balance); The type and position of the tripping device, where R stands for the pipe radius or the channel half width; The flow conditions and the flow geometry where for the channel the number gives the aspect ratio between the width and height of the channel

Two-dimensional turbulent boundary layer under zero pressure gradient

Authors	Date	$R_\theta(R_\delta) \times 10^3$	Instrument	$u_\star$ measurement	Tripping device	Free-stream turbulence	l^+
Gupta & Kaplan	1972	1.9, 6.5	HWA	$U^+ = y^+$	Trip	about 0.28%	Not given
Ueda & Hinze	1975	1.24, 4.25	HWA	$U^+ = y^+$	Trip wire	about 0.03%	2.7–6.7
Purtell et al.	1981	1.34–5.1	HWA	$U^+ = y^+$	Sand paper	below 0.05%	8.2–29.9
Azad & Burhanuddin	1983	1.68–4.81	HWA	Log-law (5.6, 5.0)	Sand paper	Not given	13–38
Blackwelder & Haritonidis	1983	1–10	HWA	$U^+ = y^+$	Rows of rivets	less than 0.2%	9–40
Schewe	1983	1.4	HWA	Not given	Not given	about 0.02%	Not given
Andreopoulos et al.	1984	3.62–15.4	HWA	$U^+ = y^+$	Not given	approx. 0.06%	20.9–83
Kunen	1984	1.75	HWA	Preston tube	Trip wire	less than 0.2%	12
Johansson et al.	1987	(2.8)	HWA	Log-law (5.62, 5.0)	Sand paper	below 0.05%	Not given
Ligrani & Bradshaw	1987	2.62	HWA	Preston tube	Not given	approx. 0.1%	3.3–16
Karlsson & Johansson	1988	2.42	LDA	$U^+ = y^+$ ($y^+ < 3$)	Screen	about 1.8%	5
Spalart	1988	3–1.41	DNS	Numerical	—	—	—
Klewicki & Falco	1990	1.01–4.85	HWA	Log-law (5.62, 5.0)	Threaded rod	less than 0.2%	1.8–7.62
Erm & Joubert	1991	5–2.8	HWA	Preston tube	Trip wire	about 0.32%	21–30
Balint et al.	1992	2.08, 2.69	HWA	Log-law (5.62, 5.0)	Trip wire	about 0.5%	7.7–10.9
Bruns et al.	1992	2.6–16.1	HWA	Preston tube	V-Dymotape	less than 0.1%	9–32
Nagano et al.	1993	1.62	HWA	Log-law (5.62, 5.0)	Row of Δ plates	below 0.1%	Not given
Nockemann et al.	1994	20.9–57.7	HWA	Preston tube	Natural	less than 0.01%	26–70
Ching et al.	1995	4, 1.32	LDA	$U^+ = y^+$ ($y^+ < 2.5$)	Pebbles	less than 1%	0.16–0.8

Fully developed internal flows

Authors	Date	$R^+(R_D) \times 10^2$	Instrument	$u_\star$ measurement	Development length (Tripping device)	Flow geometry (Aspect ratio)	l^+
Laufer	1953	5.25, 43	HWA	Pressure drop	60R (Sand paper)	Cylindrical pipe	Not given
Bakewell & Lumley	1967	(87)	HWA	Pressure drop	50R (Not given)	Cylindrical pipe	Not given
Perry & Abell	1975	23.3	HWA	Log-law (5.62, 5.0)	118R (Sand paper)	Cylindrical pipe	50–63
Kreplin & Eckelmann	1979	3.89	HWA	$U^+ = y^+$	64R (Screen)	Open channel (4)	Not given
Schildknecht et al.	1979	4.84	HWA	Pressure drop	360R (Sand paper)	Cylindrical pipe	9.7
Johansson	1982	6.7–2.06	HWA	Log-law (5.62, var.)	126R (Not given)	Rect. channel (5)	10.5–32.1
&Alfredsson	1983	2.128	HWA	Log-law (5.62, 5.0)	126R (Not given)	Rect. channel (5)	14–32
Alfredsson & Johansson	1984	7.28	HWA	$U^+ = y^+$	126R (Not given)	Rect. channel (5)	11
Kunen	1984	3.19	LDA	Pressure drop	250R (Not given)	Cylindrical pipe	4.7
Kim et al.	1987	1.8	DNS	Numerical	—	Rect. channel (–)	—
Wei & Willmarth	1989	1.69–9.89	LDA	Log-law (5.62, 5.0)	173R (Not given)	Rect. channel (12)	0.66–6.43
Niederschulte et al.	1990	1.785	LDA	$-\rho\overline{uv} + \mu\partial U/\partial y$	280R (Trip wire)	Rect. channel (12)	0.26
Antonia et al.	1992	1.8, 3.95	DNS	Numerical	—	Rect. channel (–)	—
		1.81, 2.56	HWA	Pressure drop & Preston tube	320R (Trip wire)	Rect. channel (18)	2.52–3.47
Kuroda et al.	1993	1.0	DNS	Numerical	—	Rect. channel (–)	—
Thiele & Eckelmann	1993	3.9	LDA	$U^+ = y^+$	64R (Screen)	Open channel (4)	Not given
Eggels et al.	1994	1.8	DNS	Numerical	—	Cylindrical pipe	—
		1.86	LDA	Pressure drop	268R (Perforated	Cylindrical pipe	7.6
		1.895	HWA	Pressure drop	203R plate)	Cylindrical pipe	4.0
Fontaine & Deutsch	1995	3.06	LDA	$U^+ = y^+$ ($y^+ \leq 5$)	50R (Trip wire)	Cylindrical pipe	6
Durst et al.	1995	2.4, 4.1	LDA	$U^+ = y^+$ ($y^+ \leq 2.5$)	160R (Trip)	Cylindrical pipe	2.4–6.3
den Toonder & Nieuwstadt	1996	1.69–6.9	LDA	Pressure drop	1440R (Trip ring)	Cylindrical pipe	0.83–3.46

Here, we are primarily interested in the peak value of rms of streamwise velocity fluctuations and in its dependence on the Reynolds number. This will be studied in the following subsections.

3.1 Boundary layer

First we consider a two-dimensional turbulent boundary layer under zero-pressure gradient. The data of $\sigma_u^+|_{\text{peak}}$ are depicted

Table 2. References of data over riblet walls. For further explanation see Table 1

Two-dimensional turbulent boundary layer under zero pressure gradient							
Authors	Date	$R_\theta \times 10^3$	Instrument	u_* measurement	Tripping device	Free-stream turbulence	l^+
Hooshmand et al.	1983	3.66	HWA	Log-law (5.75, var.)	Trip wire	about 0.7%	5.2
Becher & Smith	1985	1.23	HWA	Log-law (5.62, var.)	3D trip	0.4%	Not given
Vukoslavčević et al.	1987	1.0	HWA	$U^+ = y^+$	Trip wire	about 0.7%	Not given
Choi	1989	4.3	HWA	Defect law	Not given	Not given	Not given
Schwarz-van Manen et al.	1993	2.0	LDA	$U^+ = y^+$	Trip wire	Not given	Not given
Tang & Clark	1993	1.4	HWA	Log-law (5.75, 5.0) & $U^+ = y^+$ Defect law (Riblet)	Not given	Approx. 0.5%	6
de Bisschop & Nieuwstadt*	1996	5.2	HWA	Drag balance	Trip wire	Not given	Not given

*This experiment was made under an adverse pressure gradient $\beta(\equiv(\delta^*/\tau_w)\,dP/dx) = 2.2$

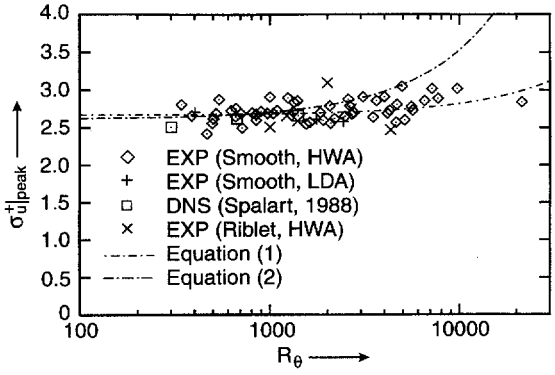

Fig. 1. Reynolds-number-dependence of the peak value of the non-dimensional rms of the streamwise velocity fluctuations in a two-dimensional turbulent boundary layer under zero pressure gradient. The data are classified according to their source and to the experimental technique used

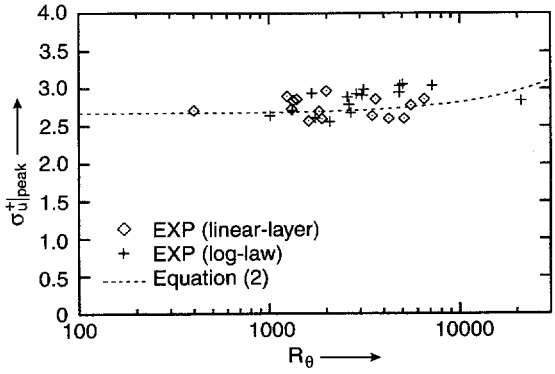

Fig. 2. Reynolds-number-dependence of the peak value of the non-dimensional rms of the streamwise velocity fluctuations in a two-dimensional turbulent boundary layer under zero pressure gradient classified according to the method by which the friction velocity is determined

in Fig. 1 as function of $R_\theta(\equiv U_\infty \theta/\nu)$ where θ is momentum thickness and U_∞ free-stream velocity. The data shown in this figure are distinguished according to their source: either DNS or experiments and for the latter also to the experimental technique Hot-Wire Anemometry (HWA) or Laser-Doppler Anemometry (LDA). For the experimental data we have used only data obtained with a reasonable instrumental resolution, i.e. the probe dimension or the maximum size of the measurement volume satisfies the condition $l^+(\equiv l u_*/\nu) < 30$ (for further details on the influence of the measuring resolution we refer to Sect. 5).

The data show at best a weak Reynolds-number dependence of $\sigma_u^+|_{peak}$, with only a slight increase as a function of the Reynolds number. However, considering the scatter in the data this trend in $\sigma_u^+|_{peak}$ is hardly significant.

The following empirical formula has been proposed by Klewicki and Falco (1990):

$$\sigma_u^+|_{peak} = 0.000092 R_\theta + 2.616 \qquad (1)$$

It is clear from Fig. 1 that it is only a reasonable fit to the data for the low Reynolds-number range. A least-squares fit to all data plotted in Fig. 1 covering the whole range $R_\theta = 300$–$20{,}920$ leads to

$$\sigma_u^+|_{peak} = 0.000015 R_\theta + 2.67 \qquad (2)$$

which shows a much smaller dependence on Reynolds number than (1). However, we again note that the slopes in both (1) and (2) can be hardly considered as statistically significant. Taking average over all the data shown in Fig. 1 we find that the peak value of σ_u^+ has a value equal to 2.71 ± 0.14.

We have mentioned above the importance of an accurate estimate for the u_*. To investigate a possible influence on our results by the procedure used to obtain u_*, we illustrate in Fig. 2 the results for $\sigma_u^+|_{peak}$ classified according to the method by which the friction velocity is determined. The classification denoted by the term "log-law" stands for experiments where u_* is obtained by a Clauser chart or with a Preston tube. These are both techniques based on universality of the law of the wall. The data marked as "linear-layer" use a u_* obtained from the slope of the linear profile observed close to the wall. The data based on the "log-law" method are on the average somewhat larger than the data based on the linear-layer method.

Moreover, they exhibit also a somewhat greater Reynolds-number dependence of $\sigma_u^+|_{peak}$. This agrees with the recent observation that use of the universal log-law would lead to an overestimate for the friction velocity at low Reynolds numbers (Ching et al. 1995). On the other hand, a reliable wall-shear stress measurement from the viscous-sublayer velocity profile is limited to very moderate Reynolds numbers. Nevertheless the small difference between the two data sets shown in Fig. 2 does not justify a correction of the $\sigma_u^+|_{peak}$ based on the measurement method of u_*.

Also, no significant difference can be found in Fig. 1 between the $\sigma_u^+|_{peak}$ data above a riblet and smooth surface, although it seems that data over a riblet surface exhibit somewhat more scatter. This equality of $\sigma_u^+|_{peak}$ above smooth and riblet walls is somewhat surprising because the drag reduction of the riblet wall could be due to modification of turbulence near the wall which would influence statistics such as rms values. One could perhaps object that an estimate of u_* above a riblet wall is difficult to measure because the universal log-wall fails here so that the indirect methods to determine u_* are useless. As a result errors in σ_u^+ might be large which would throw doubt on the significance of an equal σ_u^+-peak. Therefore, we stress that this result is primarily based on the experimental data found by deBisschop and Nieuwstadt (1996) who have used a drag balance for direct skin-friction measurements which leads to accurate data both for smooth and riblet walls.

Next we consider the location of $\sigma_u^+|_{peak}$ above the wall in terms of $y^+ (\equiv y u_*/\nu)$. The value $y^+|_{peak}$ for our data set, is plotted as a function of R_θ in Fig. 3. The figure shows all data, i.e. at all instrumental resolutions up to $l^+ = 83$ (see also Sect. 5) because l^+ does not influence the distance from the wall $y^+|_{peak}$ (Ligrani and Bradshaw 1987). In Fig. 4 the experimental data are again classified by the method according to which the friction velocity is determined, i.e. "log-law" and "linear-layer". For the data over a smooth wall, the value of $y^+|_{peak}$ scatters around 15 and seems to depend slightly on the Reynolds number with a shift away from the wall as R_θ increases. A mean value of $y^+|_{peak}$ over all data is 14.9 with a standard deviation of 1.31 (8.8% of its mean value).

A least-squares fit to the data leads to

$$y^+|_{peak} = 0.00017 R_\theta + 14.4 \qquad (3)$$

It follows from a comparison of the slope in (3) with the slope given in (2) that the $y^+|_{peak}$ depends somewhat stronger on R_θ than the $\sigma_u^+|_{peak}$.

For the data above the riblet surface we find a large scatter in the value of $y^+|_{peak}$. This is most probably due to the fact that the origin of the y-axis is difficult to determine above a riblet surface. The mean value of $y^+|_{peak}$ above a riblet surface is about 23. This value implies that the hypothesis which assumes $y^+|_{peak} = 15$ to be universally valid both over riblet and smooth surfaces, is probably not correct. Thus, such hypothesis is not suitable to determine the virtual origin over a riblet surface (Choi et al. 1993).

3.2 Internal flow

In Fig. 4 we show the results on $\sigma_u^+|_{peak}$ for fully developed two-dimensional channel and cylindrical pipe flows. The Reynolds number is defined in this case as $R^+ \equiv u_* R/\nu$ where R is the pipe radius or the half-width of channel height. Only the experimental data which satisfy the condition $l^+ < 30$ (see Sect. 5) are plotted in this figure. It is clear that $\sigma_u^+|_{peak}$ is almost constant with quite small scatter over the whole Reynolds-number range between $R^+ = 100$–4,300. A least-squares fit to all data leads to

$$\sigma_u^+|_{peak} = -0.0000024 R^+ + 2.70 \qquad (4)$$

and this clearly shows the very small Reynolds-number dependence.

Furthermore, the data on $\sigma_u^+|_{peak}$ do not seem to depend on the size of the flow domain in the spanwise direction. For instance, values for channel flows with different aspect ratios between the channel height and width (see Table 1) have been plotted in Fig. 4 with no noticeable difference in $\sigma_u^+|_{peak}$.

The mean value of $\sigma_u^+|_{peak}$ taken over all data is 2.70 with a standard deviation of 0.087 (3.2% of its mean value). This is very close to the corresponding value for the boundary layer (the difference is statistically not significant).

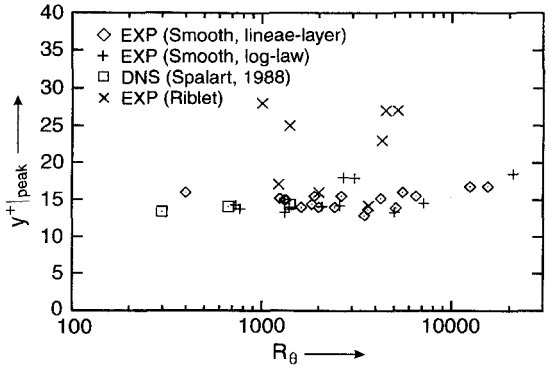

Fig. 3. Reynolds-number-dependence of normalised distance from the wall where σ_u^+ has a maximum value for the case of a two-dimensional turbulent boundary layer under zero pressure gradient. The data are classified according to their source and to the technique used to obtain u_*

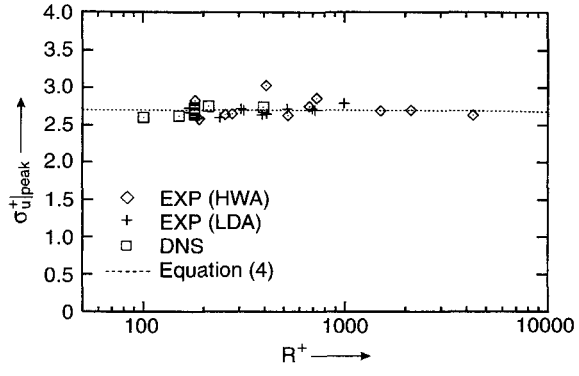

Fig. 4. Reynolds-number-dependence of the peak value of non-dimensional rms of the streamwise velocity fluctuations in fully developed two-dimensional channel and pipe flows. The data are classified according to their source and to the experimental technique

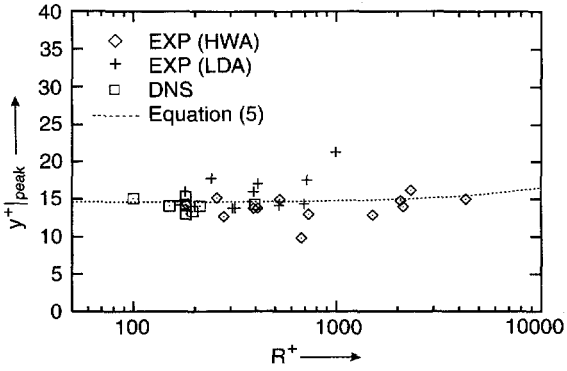

Fig. 5. Reynolds-number-dependence of normalised distance from the wall where σ_u^+ takes a maximum value in fully developed two-dimensional channel and pipe flows. The data are classified according to their source and the experimental technique

The data of $y^+|_{peak}$ for the case of internal flows are shown in Fig. 5. The scatter in the data is rather large so that it is difficult to draw a conclusion on the dependence of $y^+|_{peak}$ as a function of the Reynolds number. Nevertheless, a weak Reynolds-number-dependence seems to be apparent. A least-squares linear fit to all data gives the following expression:

$$y^+|_{peak} = 0.00020R^+ + 14.6. \quad (5)$$

3.3 Discussion

We have found that both for boundary-layer and in internal (pipe and channel) flows the peak value in the rms of the streamwise velocity fluctuations is equal and moreover independent of the Reynolds number. This may be compared with other variables, such as the constants in the logarithmic velocity profile. These are found to exhibit significant Reynolds dependence (Wei and Willmarth 1989; Ching et al. 1995; den Toonder and Nieuwstadt 1996). Moreover, the fact that the value of $\sigma_u^+|_{peak}$ is independent of the flow geometries such as a boundary layer or internal flow, suggests that the streamwise velocity fluctuations are in equilibrium with the local wall shear stress. This seems to imply that near-wall streamwise velocity fluctuations are determined by so-called "active" motion which are supposed to be in equilibrium with the wall shear stress. However, this is in contradiction with the hypothesis that streamwise velocity fluctuations are also influenced by so-called "inactive" motions which result from the outer layer (Bradshaw 1967). These "inactive" motions are not necessarily in equilibrium with the local wall shear stress and furthermore they are likely to depend on the flow geometry so that one would expect the "inactive" motions to be different for boundary layer and internal flows. In other words the constancy of $\sigma_u^+|_{peak}$ throws doubts on the role of inactive motions near the wall and at the same time gives support to inner-layer scaling which is based on the assumption of equilibrium of near-wall turbulence with its surface parameters. However, it should be also mentioned that all aspects of inner-layer scaling and its applicability are still far from being completely clear (Bradshaw and Huang 1995).

Nevertheless, the constant value that we found for $\sigma_u^+|_{peak}$, seems to be an experimental fact and this can be put to good use for a number of applications. For instance, one can use this result to determine the wall-shear stress from the observations of the streamwise velocity fluctuations. An estimate based on a second-order quantity such as a rms-value would perhaps seem less accurate due to statistical error than an estimate based on a first-order quantity such as a mean logarithmic velocity profile. The wall-shear stress estimate based on streamwise velocity fluctuations would, however, be preferable in cases where the constants in the logarithmic profile are not well known. This is for instance the case in low Reynolds-number conditions because the constants in the logarithmic profile are known to be highly Reynolds-number dependent. The method to obtain wall-shear stress from streamwise velocity fluctuations can be also extended to riblet walls where the logarithmic profile is not known because its constants depend directly on the obtained skin-friction reduction.

Furthermore, we expect the constant value of $\sigma_u^+|_{peak}$ as function of Reynolds number to be a good test for turbulence models designed for low-Reynolds-number wall flows.

4 Skewness at $y^+|_{peak}$

In this section we consider the third-order moment of streamwise velocity fluctuations at $y^+|_{peak}$, i.e. at the position where the rms of the streamwise velocity fluctuations has its maximum value. This third-order moment can be expressed in dimensionless form as the skewness, $S_u = \overline{u'^3}/(\overline{u'^2})^{3/2}$. The values for S_u at $y^+|_{peak}$ are shown in Fig. 6 for the boundary layer and in Fig. 7 for the internal flows. Only the experimental data which have sufficient instrumental resolution, $l^+ < 30$, are plotted in these figures. It follows that the value of S_u at $y^+|_{peak}$ is constant over the moderate Reynolds number ranges, $R_\theta = 730$–$6{,}500$ in the boundary layer and $R^+ = 150$–$2{,}128$ in the internal flows. Moreover, this constant value appears to be equal to zero.

This latter result can be supported by considering the equation for third-order moment, $\overline{u'^3}$. With the assumptions of

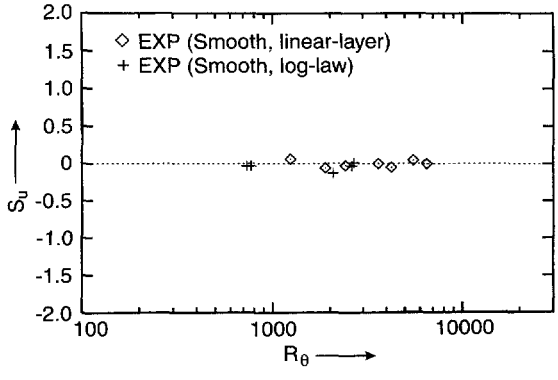

Fig. 6. Reynolds-number-dependence of S_u at $y^+|_{peak}$ in a two-dimensional turbulent boundary layer under zero pressure gradient. The data are classified according to method used to obtain the wall shear stress

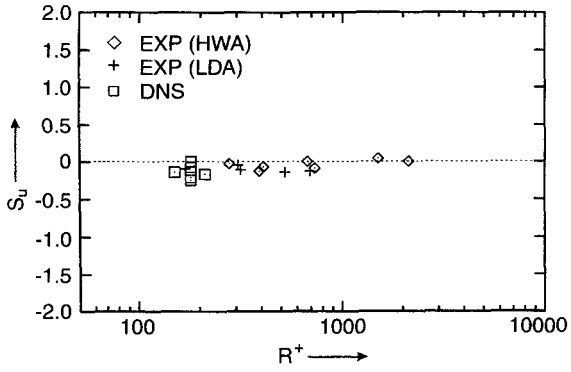

Fig. 7. Reynolds-number-dependence of S_u at $y^+|_{peak}$ in fully developed two-dimensional channel and pipe flows. The data are classified according to the source and the experimental technique

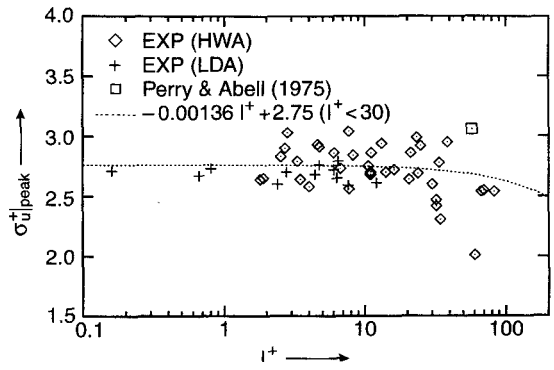

Fig. 8. Influence of imperfect spatial resolution on the peak value $\sigma_u^+|_{peak}$. The data are classified according to the experimental technique

horizontal homogeneity and negligible viscous terms, this equation reduces to

$$0 = \overline{u'^2}\frac{\partial \overline{u'v'}}{\partial y} - \overline{u'^2 v'}\frac{\partial \bar{u}}{\partial y} - \frac{1}{3}\frac{\partial \overline{u'^3 v'}}{\partial y} - \frac{1}{\rho}\overline{u'^2}\frac{\partial \overline{p'}}{\partial x} \tag{6}$$

where the first two terms on the right-hand side are production terms. With the additional assumption of Gaussian turbulence, which is consistent with a zero third-order moment being close to zero, it follows that the second production term is zero and also that $\overline{u'^3 v'} = 3\overline{u'v'}\,\overline{u'^2}$. If we furthermore estimate the pressure term as $\overline{u'^3}/\mathcal{T}$ where $\mathcal{T}$ is a turbulent time scale, we find

$$\overline{u'^3} = -\mathcal{T}\,\overline{u'v'}\frac{\partial \overline{u'^2}}{\partial y}. \tag{7}$$

This result confirms that the zero value of the third-moment should coincide with the maximum value of the second-order moment. Although this result may seem restricted by the strong assumptions that we had to make, we can refer to Jovanovic et al. (1993) who come to the same conclusion based on a more general consideration of the higher-order moment equations.

The result found above is also a confirmation of the turbulence models which estimate the third-order transport terms by (Hanjalić and Launder 1972)

$$\overline{u_i' u_j' u_k'} \simeq \overline{u_k' u_l'}\frac{\partial \overline{u_i' u_j'}}{\partial x_l}. \tag{8}$$

5
Influence of instrumental resolution

The influence of the instrumental resolution on turbulence measurements has been examined by several authors with help of their own experimental facility (see e.g. Johansson and Alfredsson 1983; Ligrani and Bradshaw 1987). Gad-el-Hak and Bandyopadhyay (1994) give as a criterion that the Reynolds number based on a measuring dimension, l^+, should be less than 5 for accurate turbulence measurements. To check this criterion and also to estimate the effect of instrumental resolution on $\sigma_u^+|_{peak}$, we show in Fig. 8 the values of $\sigma_u^+|_{peak}$ as a function of l^+. We distinguish in this figure between ex-

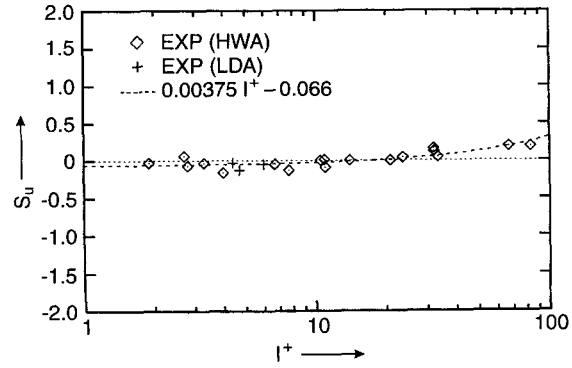

Fig. 9. Influence of imperfect spatial resolution on S_u at $y^+|_{peak}$. The data are classified according to the experimental technique

periments performed by HWA and LDA. It appears that the HWA measurements exhibits more scatter than the LDA data. This can possibly be explained by errors due to the more complicated calibration procedure for HWA respect to LDA (see also Perry and Abell, 1975).

Figure 8 shows that the value of $\sigma_u^+|_{peak}$ stays about constant up to $l^+ \simeq 30$ and thereafter slowly decreases. This decrease is due to the filtering effect by the large measuring volume. A similar result is found for the values of the skewness S_u at $y^+|_{peak}$ plotted as a function of l^+, shown in Fig. 9. In this case, we find that for $l^+ > 30$ the S_u departs significantly from zero.

Based on these results we propose that a critical value of l^+ for reasonably accurate measurements of the streamwise fluctuations can be set at about 30. This value is somewhat greater than the value of 20–25 proposed by Ligrani and Bradshaw (1987).

6
Summary and conclusion

In this study we have focused on the peak value in the profile of the rms of streamwise velocity fluctuations. In particular we have considered the Reynolds number dependence of this peak value for both boundary layer and internal flows (i.e. a pipe and channel). Based on a number of experimental data (both over smooth and riblet surfaces) and direct-simulation results,

we have found that this peak value is constant as a function of the Reynolds number within the scatter of the data. The value is 2.71 ± 0.13 for a range of Reynolds numbers between $R_\theta = 300$–$20{,}920$ for the boundary layer and $R^+ = 100$–$4{,}300$ for the internal flows. The location of the peak value, $y^+|_{\text{peak}}$, was found to be slightly dependent on the Reynolds number. Moreover, we find that the value of the skewness at the location $y^+|_{\text{peak}}$ is equal to zero independent of the Reynolds number again within experimental scatter. This result is consistent with an expression which follows from a simplification of the third-order moment equation.

The fact that the value of $\sigma_u^+|_{\text{peak}}$ is the same both for boundary layer and internal flows suggests that in the near-wall region the streamwise velocity fluctuations are in local equilibrium with the wall-shear stress. This seems to be in contradiction with the notion that streamwise velocity fluctuations are influenced by so-called "inactive" motions which have their origin in the outer layer.

Apart from the dynamical consequences of the constant value of $\sigma_u^+|_{\text{peak}}$ as function of the Reynolds number, this result can be put to use, e.g. to estimate of the friction velocity from measurements of the streamwise velocity fluctuations. This procedure should be useful in particular for those situations where other methods, e.g. those based on the mean velocity profile, are known to fail. Examples are flows with low Reynolds number and flows over a riblet surface.

As a last remark, it should be mentioned that all our data have been obtained for a smooth wall (apart from the riblet surface which is a rather special case). The streamwise velocity fluctuations above a rough wall are not as well documented as for the smooth wall. However, some first examination of data sets obtained above a rough wall suggests that the values of the near-wall rms of the streamwise velocity fluctuations are quite comparable with the results found here but a clear maximum value is in general not observed in that case. Nevertheless, the ultimate test of the ideas put forward in this paper would be to carry out an experiment in a near-wall turbulent flow at very large Reynolds numbers. An experiment in the atmospheric boundary layer could be a candidate. The data for this boundary layer, published for instance by Panofsky and Dutton (1984, p. 160), give for the near-surface σ_u^+ the value 2.39. However, it should be mentioned that most atmospheric measurements are carried at heights above the surface ≥ 10 m which may explain the lower values compared to our result of 2.71.

References

Alfredsson PH; Johansson AV (1984) On the detection of turbulent-generating events. J Fluid Mech 139: 325–345

Andreopoulos J; Durst F; Zaric Z; Javanović J (1984) Influence of Reynolds number on characteristics of turbulent wall boundary layers. Exp Fluids 2: 7–16

Antonia RA; Teitel M; Kim J; Browne LWB (1992) Low-Reynolds number effects in a fully developed turbulent channel flow. J Fluid Mech 236: 579–605

Azad RE; Burhanuddin S (1983) Measurements of some features of turbulence in wall-proximity. Exp Fluids 1: 149–160

Bakewell HP; Lumley JL (1967) Viscous sublayer and adjacent wall region in turbulent pipe flow. Phys Fluids 10: 1880–1889

Balint J-L; Wallace JM; Vukoslavčević P (1992) The velocity and vorticity vector fields of a turbulent boundary layer: Part 2: Statistical properties. J Fluid Mech 228: 53–86

Becher EV; Smith CR (1985) A combined visualisation-anemometry study of the turbulent drag reducing mechanisms of triangular micro-groove surface modification. AIAA Paper 85-0548

Blackwelder RF; Haritonidis JH (1983) Scaling of the bursting frequency in turbulent boundary layers. J Fluid Mech 132: 87–103

Bradshaw P (1967) "Inactive" motion and pressure fluctuations in turbulent boundary layers. J Fluid Mech 30: 241–258

Bradshaw P; Huang GP (1995) The law of the wall in turbulent flows. Proc R Soc Lond A 451: 165–188

Bruns J; Dengel P; Fernholz HH (1992) Mean flow and turbulence measurements in an incompressible turbulent boundary layer. Part 1: Data. Institutsbericht Nr. 02/92, Harmann-Föttinger-Institut für Thermo- und Fluiddynamik, Technische Universität Berlin

Ching CY; Djenidi L; Antonia RA (1995) Low-Reynolds-number effects in a turbulent boundary layer. Exp Fluids 19: 61–68

Choi H; Moin P; Kim J (1993) Direct numerical simulation of turbulent flow over riblets. J Fluid Mech 255: 503–539

Choi K-S (1989) Near-wall structure of turbulent boundary layers over smooth and riblet surfaces. J Fluid Mech 208: 417–458

Coles D (1956) The law of the wake in the turbulent boundary layer. J Fluid Mech 1: 191–226

Dean RB (1978) Reynolds number dependence of skin friction and other bulk flow variables in two-dimensional rectangular duct flow. Trans ASME, J Fluids Eng 100: 215–223

deBisschop JR; Nieuwstadt FTM (1995) A turbulent boundary layer in an adverse pressure gradient: The effectiveness of riblets. AIAA J (in press)

den Toonder JMJ; Nieuwstadt FTM (1996) Reynolds number effects in a turbulent pipe flow for low to moderate *Re*. (submitted to Physics of Fluids)

Dussauge J-P; Fernholtz HH; Finley PJ; Smith RW; Smits AJ; Spina EF (1995) Turbulent boundary layers in subsonic and supersonic flow. AGARDograph 335

Durst F; Jovanović J; Sender J (1995) LDA measurements in the near wall region of a turbulent pipe flow. J Fluid Mech 295: 305–339

Durst F; Kikura H; Lekakis I; Jovanović J; Ye Q (1996) Wall shear stress determination from near-wall mean velocity data in turbulent pipe and channel flows. Unpublished manuscript

Eggels JGM; Unger F; Weiss MH; Westerweel J; Adrian RJ; Friedrich R; Nieuwstadt FTM (1994) Fully developed turbulent pipe flow: a comparison between direct numerical simulation and experiment. J Fluid Mech 268: 175–209

Erm LP; Joubert PN (1991) Low-Reynolds-number turbulent boundary layers. J Fluid Mech 230: 1–44

Fontaine AA; Deutsch S (1994) Three-component, time-resolved velocity statistics in the wall region of a turbulent pipe flow. Exp Fluids 18: 168–173

Gad-el-Hak M; Bandyopadhyay PR (1994) Reynolds number effects in wall-bounded turbulent flows. Appl Mech Rev 47: 307–365

Gupta AK; Kaplan RE (1972) Statistical characteristics of Reynolds stress in a turbulent boundary layer. Phys Fluids 15: 981–985

Hanjalić K; Launder BE (1972) A Reynolds stress model of turbulence and its application to thin shear flows. J Fluid Mech 52: 609–638

Hinze JO (1975) Turbulence. 2nd edition, McGraw-Hill

Hooshmand A; Youngs RA; Wallace JM; Balint J-L (1983) An experimental study of changes in the structure of a turbulent boundary layer due to surface geometry changes. AIAA Paper 83-0230

Johansson AV; Alfredsson AV (1982) On the structure of turbulent channel flow. J Fluid Mech 122: 295–314

Johansson AV; Alfredsson AV (1983) Effects of imperfect spatial resolution on measurements of wall-bounded turbulent shear flows. J Fluid Mech 137: 409–421

Johansson AV; Her J-Y; Haritonidis JH (1987) On the generation of high-amplitude wall-pressure peaks in turbulent boundary layers and spots. J Fluid Mech 175: 119–142

Jovanovic J; Durst F; Johansson TG (1993) Statistical analysis of the dynamical equations for higher-order moments in turbulent wall bounded flows. Phys Fluids A5: 2886–2900

Karlsson RI; Johansson TG (1988) LDV measurements of higher order moments of velocity fluctuations in a turbulent boundary layer. In: Laser anemometry in fluid mechanics III (eds. R. J. Adrian, T. Asanuma, D. F. G. Durão, F. Durst and J. H. Whitelaw), Lisbon, Portugal: 273–289

Kim J; Moin P; Moser R (1987) Turbulence statistics in fully developed channel flow at low Reynolds number. J Fluid Mech 177: 133–166

Klewicki JC; Falco RE (1990) On accurately measuring statistics associated with small-scale structure in turbulent boundary layers using hot-wire probes. J Fluid Mech 219: 119–142

Kunen JMG (1984) On the detection of coherent structures in turbulent flows. Ph.D. Thesis Delft University of Technology

Kuroda A; Kasagi N; Hirata M (1993) Direct numerical simulation of the turbulent Cuette-Poiseulle flows: Effect of mean shear on the near wall turbulence structures. In: Ninth Symposium on Turbulent Shear Flows (eds. F. Durst, N. Kasagi, B. E. Launder, F. W. Schmidt, K. Suzuki and J. H. Whitelaw), Springer-Verlag, 241–257

Kreplin H-P; Eckelmann H (1979) Behaviour of the three fluctuating velocity components in the wall region. Phys Fluids 22: 1233–1239

Laufer J (1953) The structure of turbulence in fully developed pipe flow. NACA Report 1174

Ligrani PM; Bradshaw P (1987) Spatial resolution and measurement of turbulence in the viscous sublayer using subminiature hot-wire probes. Exp Fluids 5: 407–417

Murlis J; Tsai HM; Bradshaw P (1981) Structure of turbulent boundary layers at low Reynolds numbers. J Fluid Mech 122: 13–56

Nagano Y; Tagawa M; Tsuji T (1993) Effects of adverse pressure gradients on mean flows and turbulence statistics in a boundary layer. In: Eighth Symposium on Turbulent Shear Flows (eds. F. Durst, R. Friedrich, B. E. Launder, F. W. Schmidt, U. Schumann and J. H. Whitelaw), Springer-Verlag, 7–12

Niederschulte MA; Adrian RJ; Hanratty TJ (1990) Measurements of turbulent flow in a channel at low Reynolds numbers. Exp Fluids 9: 222–230

Nockemann M: Abstiens R; Schober M; Bruns J; Eckert D (1994) Vermessung der Wandgrenzschicht im Deutsch-Niederländischen Windkanal bei hohen Reynolds-zahlen. Institutsreport, Aerodynamisches Institut RWTH Aachen

Panofsky HA; Dutton JA (1984) Atmospheric Turbulence; Models and Methods for Engineering Applications. New York: Wiley

Perry AE; Abell CJ (1975) Scaling laws for pipe-flow turbulence. J Fluid Mech 67: 257–271

Purtell LP; Klebanoff PS; Buckley FT (1981) Turbulent boundary layer at low Reynolds number. Phys Fluids 24: 802–811

Schewe G (1983) On the structure and resolution of wall-pressure fluctuations associated with turbulent boundary-layer flow. J Fluid Mech 134: 311–328

Schildknecht M; Miller JA; Meier GEA (1979) The influence of suction on the structure of turbulence in fully developed pipe flow. J Fluid Mech 90: 67–107

Schwarz-van Manen AD; Geloven AFM; Nieuwenhuizen J; Stouthart JC; Prasad KK; Nieuwstadt FTM (1993) Friction velocity and virtual origin estimates for mean velocity profiles above smooth and triangular riblet surfaces. Appl Sci Res 50: 233–254

Spalart PR (1988) Direct simulation of a turbulent boundary layer up to $R_\theta = 1410$. J Fluid Mech 187: 61–98

Tang YP; Clark DG (1993) On near-wall turbulence-generating events in turbulent boundary layer over a riblet surface. Appl Sci Res 50: 215–232

Tennekes H; Lumley JL (1972) A first course in turbulence. The MIT Press

Thiele B; Eckelmann H (1993) Application of a partly submerged two component laser-doppler anemometer in a turbulent flow. Exp Fluids 17: 390–396

Ueda H; Hinze JO (1975) Fine structure turbulence in the wall region of a turbulent boundary layer. J Fluid Mech 67: 125–143

Vukoslavčević P; Wallace JM; Balint J-L (1987) On the mechanism of viscous drag reduction using streamwise allined riblets: A review with new results. Turbulent drag reduction by passive means (Three days international conference), Vol. 2, The Royal Aeronautical Society, London: 290–309

Wei T; Willmarth WW (1989) Reynolds number effects on the structure of a turbulent channel flow. J Fluid Mech 204: 57–95